Anal Bioanal Chem (2010) 398:1919–1925
DOI 10.1007/s00216-010-4127-4

ORIGINAL PAPER

Application of FLIM-FIDSAM for the in vivo analysis of hormone competence of different cell types

Kirstin Elgass · Katharina Caesar · Dierk Wanke · Klaus Harter · Alfred J. Meixner · Frank Schleifenbaum

Received: 7 June 2010 / Revised: 11 August 2010 / Accepted: 11 August 2010 / Published online: 2 September 2010

Abstract Background fluorescence derived from subcellular compartments is a major drawback in high-resolution live imaging, especially of plant cells. A novel technique for contrast enhancement of fluorescence images of living cells expressing fluorescent fusion proteins termed fluorescence intensity decay shape analysis microscopy (FIDSAM) has been recently published and is applied here to plant cells expressing wild-type levels of a low-abundant membrane protein (BRI1-EGFP), demonstrating the applicability of FIDSAM to samples exhibiting about 80% autofluorescence. Furthermore, the combination of FIDSAM and fluorescence lifetime imaging microscopy enables the simultaneous determination and quantification of different ligand-specific responses in living cells with high spatial and temporal resolution even in samples with high autofluorescence background. Correlation of different responses can be used to determine the hormone ligand competence of different cell types as demonstrated here in BRI1-EGFP-expressing root and hypocotyl cells.

Published in the special issue *Optical Biochemical and Chemical Sensors (Europtrode X)* with guest editor Jiri Homola.

Electronic supplementary material The online version of this article (doi:10.1007/s00216-010-4127-4) contains supplementary material, which is available to authorized users.

K. Elgass · A. J. Meixner
Institute of Physical and Theoretical Chemistry,
University of Tübingen,
Auf der Morgenstelle 8,
72076 Tübingen, Germany

K. Caesar · D. Wanke · K. Harter · F. Schleifenbaum (✉)
Center for Plant Molecular Biology,
Department of Plant Physiology, University of Tübingen,
Auf der Morgenstelle 1,
72076 Tübingen, Germany
e-mail: frank.schleifenbaum@uni-tuebingen.de

Keywords FIDSAM · Membrane-potential sensor · Endogenous expression · Fluorescence lifetime · EGFP · BRI1

Introduction

Increased spatial resolution beyond Abbe's diffraction limit is one of the most essential aims in optical microscopy to be reported in recent literature. Several approaches aiming to overcome this limit have been established using, e.g., short laser pulses (stimulated emission depletion microscopy, STED) [1, 2] or single molecule blinking statistics (photo-activated localization microscopy, PALM) [3]. However, biological organisms often exhibit a considerable autofluorescence background, which corrupts the contrast of fluorescence images. Therefore, a crucial aim in the development of new microscopic techniques is suppression of autofluorescence background and therewith contrast enhancement of fluorescence intensity images.

Other than in animal field, live-cell imaging of plant cells suffers especially from autofluorescence background, which spectrally overlaps with the emission of commonly used marker dyes [4] such as (auto)fluorescent proteins (AFPs). Hence, a discrimination using appropriate spectral filters does not lead to satisfying results [5]. To overcome this restriction, we recently established a novel approach to suppress autofluorescence interference in fluorescence images of living cells by fluorescence decay shape analysis microscopy (FIDSAM) [6].

Conventional ways to overcome the background fluorescence problem in plant cells often utilize the overexpression of AFP fusion proteins to enhance the intensity signal beyond the autofluorescence level. However, mis- or overexpression can lead to intracellular mislocalization and, thus, might also

interfere with the in vivo function of the fusion protein by interfering, for instance, with unrelated signal response pathways. Therefore, a desirable aim in plant fluorescence microscopy is the investigation of AFP fusion proteins expressed under their native promoter, meaning that the expression level and intracellular localization of the investigated protein reflect those of wild-type cells. However, cells expressing a low-abundant AFP fusion protein from a genomic fragment including its native promoter are the most challenging biological samples for fluorescence microscopy as these cells exhibit a very low amount of labeled proteins, and, hence, the AFP fluorescence is very often outshined by the autofluorescence background.

The excited state lifetime of autofluorescent proteins such as the enhanced green fluorescent protein (EGFP) depends on several parameters in its close physico-chemical environment such as the pH value and the membrane potential [5, 7–15]. Therefore, the monitoring of the fluorescence lifetime (FLT) can be used as a non-invasive readout for the intracellular nano-environment of the EGFP fusion protein.

We demonstrated the changes of the FLT for changed membrane potentials for the example of the plasma membrane-bound BRI1 protein. BRI1 is a receptor for plant steroid hormones such as brassinolide (BL) [16], which recycles through endosomes [17]. In early plant life, BL-dependent BRI1 signal transduction is involved in the regulation of many aspects of growth and differentiation, including cell expansion [18, 19]. Up to now, the sensitivity of BRI1-EGFP as an in vivo sensor for the membrane potential could only be recorded at selected compartments. However, a microscopy image mapping the membrane potential and its distribution over a complete cell has not been shown. This is mainly due to the fact that the expression level of BRI1 is very low so that autofluorescence cross-talk cannot be excluded and thus a quantitative study is adulterated.

The combination of the FIDSAM technique with the BRI1-EGFP membrane-potential readout should enable the mapping of different ligand-specific responses (here, (1) FLT decrease of BRI1-EGFP and (2) cell-wall expansion [5]) at subcellular level with a high spatial and temporal resolution even in samples with high autofluorescence background. This is demonstrated here by the use of transgenic *Arabidopsis* seedlings expressing wild-type levels of BRI1-EGFP, as an example [17].

Results and discussion

FIDSAM analysis of low-abundant BRI1-EGFP in living plant cells

To date, the ability of FIDSAM has been demonstrated for low-abundant, albeit still overexpressed plant proteins. Therefore, we used a transgenic *Arabidopsis* line ectopically overexpressing BRI1-EGFP. By investigating a plant line with expression levels that reflect that of endogenous BRI1 protein [17]c we now excluded overexpression artifacts. Hence, the BRI1-EGFP transformats are a valuable object to inspect the ability of FIDSAM, as the experimental results can directly be compared to one another.

To further determine the methodical limitation of FIDSAM and to judge the capability of this method, we first determined the actual signal-to-autofluorescence ratio via fluorescence spectroscopy and subsequently applied FIDSAM to recorded fluorescence lifetime imaging microscopy (FLIM) images from living, transgenic *Arabidopsis* cells.

Therefore, we recorded fluorescence spectra in leaf and hypocotyl cells of transgenic *Arabidopsis thaliana* seedlings transgenic for a P_{BRI1}::*BRI1-EGFP* construct, which expresses BRI1-EGFP to wild-type level [17] (Fig. 1a: green circles). Reference measurements were recorded in wild-type plants (100% autofluorescence) (orange line) and from purified EGFP (concentration $c = 10^{-6}$ M in pH=8.8 TRIS buffer solution) (green line). Calculating the label-to-autofluorescence ratio by integration over both spectra results in a simulated fluorescence spectrum (black line) that adequately matches the recorded spectrum (green circles). Note that the upper integration limit was set to 590 nm, excluding all fluorescence that is originating from chloroplasts and only taking into account the autofluorescence, which is derived from other cellular compartments such as the cell wall (Electronic Supplementary Material Fig. S1). The calculation revealed that 20% EGFP fluorescence and 80% autofluorescence contributed to the total fluorescence of the BRI1-EGFP-expressing cells (Fig. 1b).

We applied FIDSAM to FLIM images of BRI1-EGFP accumulating root cells, which were treated with 50 nM BL, a specific hormone ligand of BRI1. The original FLIM images revealed a decrease of the FLT of membrane-located BRI1-EGFP within 30 min after BL application (Fig. 2a–c). This decrease was also observed in the FLIM images corrected by FIDSAM (Fig. 2d–f). However, the FIDSAM correction significantly increased the dynamic contrast and suppressed the autofluorescence contribution of several intracellular compartments (see orange circles in Fig. 2) whereas the BRI1-EGFP labeled cell membranes and intracellular vesicles (yellow circles) are well preserved. These data indicate the coexistence of BRI1-EGFP-containing vesicles next to unspecific autofluorescent vesicles. Conclusively, FIDSAM is applicable to study low-abundant (membrane) AFP fusion proteins, where the AFP fluorescence contribution to the overall fluorescence is 20% or less (unpublished).

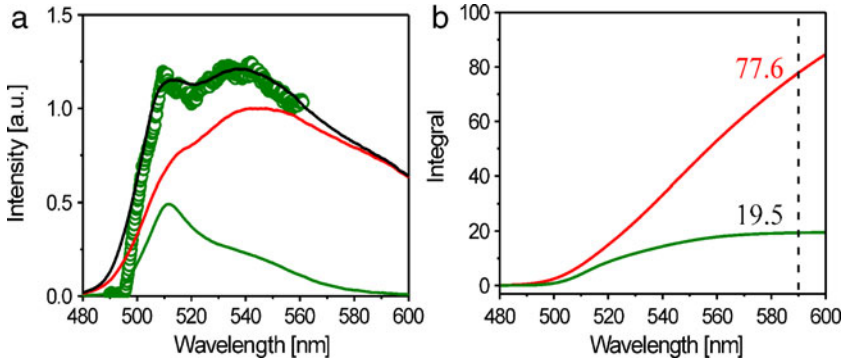

Fig. 1 GFP fluorescence-to-autofluorescence ratio in transgenic *Arabidopsis* plant cells expressing BRI1-EGFP from a genomic fragment [17]. **a** Fluorescence spectrum recorded in BRI1-EGFP-expressing leaf cells (*green circles*). The reference spectrum of 100% autofluorescence (*red line*) was recorded in leaf cells of wild-type plants. The reference spectrum of 100% EGFP fluorescence (*green line*) was obtained from purified EGFP (concentration, 10^{-6} M in pH 8.8 TRIS buffer solution). Summation over both spectra results in a simulated fluorescence spectrum (*black line*) that adequately matches the recorded spectrum (*green circles*). **b** Integration over the autofluorescence spectrum (*red line*) and the EGFP spectrum (*green line*) shown in **a**. The upper integration limit was set to 590 nm (*dotted line*)

Membrane-potential mapping with high spatial resolution

The FIDSAM-FLIM images of untreated plant cells (no BL addition) (Figs. 2a, d and 4a, d; Electronic Supplementary Material Fig. S2a and S2d) revealed differences in the FLT of BRI1-EGFP and, thus, in the local membrane potential, which is indicative of a spatially highly organized dependence of the membrane potential in different domains within plasma membranes. Interestingly, after application of BL, the FLT decrease in response to BL treatment occurred on a faster time scale in some domains within the plasma membrane (blue squares in Fig. 2, the corresponding lifetimes are given on the right side of the figure). This suggests a highly ordered function of BRI1-containing protein complexes, which are formed in vivo [20].However, 30 min after application of BL, the FLT of BRI1-EGFP has equalized to a defined minimum in all analyzed membrane domains, suggesting an active regulation, which limits hyperpolarization of the plasma membranes to a maximum value. Obviously, the membrane potential cannot exceed a certain level, which indicates the existence of counteracting mechanisms that restrict very high membrane potentials. These mechanisms protect the plasma membranes from extreme hyperpolarization, which could interfere with the vital, physiological processes such as ion and nutrient transport and the activity of many plasma membrane-located proteins and enzymes [21–27].

Hormone ligand competence depends on the cell type

The FLT decrease of BRI1-EGFP is paralleled by a cell-wall expansion [5], which might be attributed to an acidification of the apoplastic space [20] by the P-ATPase. The acidification of the apoplast probably contributes to the loosening of the cell-wall matrix and, thus, allows for the initiation of the growth process [19, 20].

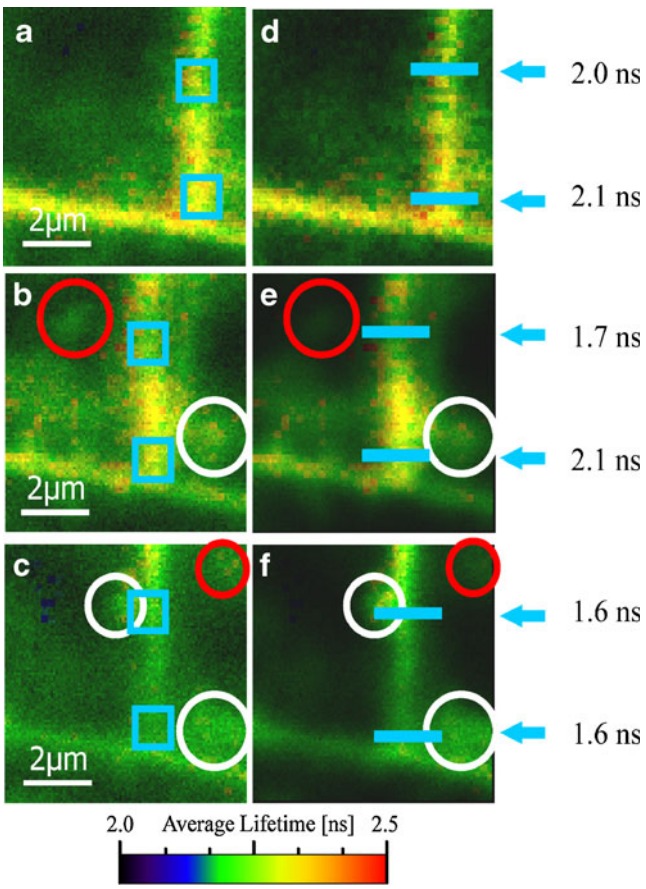

Fig. 2 BL-induced fluorescence lifetime decrease in BRI1-EGFP-expressing root cells monitored by FLIM and FIDSAM-FLIM. **a–c** FLIM images of BRI1-EGFP-expressing root cells before (**a**), 15 min (**b**), and 30 min (**c**) after addition of 50 nM BL. **d–f** FIDSAM-FLIM images of BRI1-EGFP-expressing leaf cells before (**d**), 15 min (**e**) and 30 min (**f**) after BL addition

In the membrane-labeled plant cells, the local cell-wall width can be monitored by calculating the full width at half maximum of Gaussian fittings to fluorescence intensity profiles across plasma membrane cell-wall sections (as indicated by the white lines in Fig. 2) [5].

By plotting the local FLT of BRI1-EGFP against the corresponding cell-wall width as derived from the FIDSAM-FLIM images, a linear relationship of both was revealed. Figure 3 shows four independent single-cell measurements, two recorded in root cells (gray and blue squares) and two recorded in hypocotyl cells (red and green circles). The *y* error bars represent the lifetime error given by the temporal resolution of the microscope (channel width=32 ps). The *x* error bars represent the error of the corresponding Gaussian fit [5]. The single-cell measurements cannot be plotted as average values due to the strong varieties between individual cells [5]. Former experiments disclosed a dependence of the degree of cell-wall expansion on its orientation within the cell (periclinal or anticlinal) [5]. To avoid influences of the cell-wall orientation, all the following experiments were performed at anticlinal cell walls.

The degree of cell-wall expansion is reflected by the slope of the corresponding linear fit. Therefore, this slope denotes a measure for the local competence of the cells to respond to a ligand. By applying the slope of the linear fits to the data presented here and to previous measurements [5, 20], we revealed a higher BL competence in BRI1-EGFP-expressing hypocotyl cells than in root cells. Possible explanations for the unequal BL competence in the different cell types are plentiful and may include different compositions of the cell walls, different P-ATPase efficiencies in the corresponding cells, or differing numbers of downstream effector proteins that influence microtubule orientation or the degree of cross-linking of the cell-wall matrix. Hence, further experiments are required to settle this question.

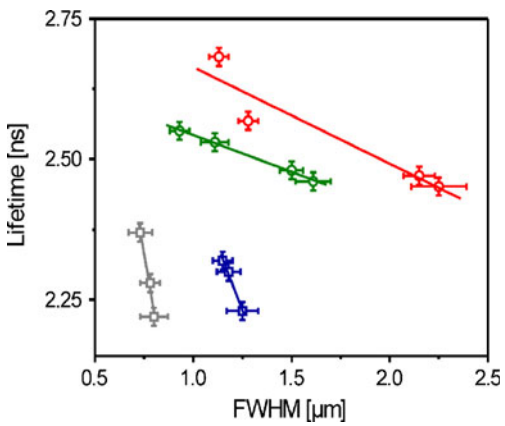

Fig. 3 Competence of different cell types to respond to the hormone ligand BL. A linear relationship between the local FLT of BRI1-EGFP and the corresponding cell-wall width could be observed in root cells (*gray* and *blue squares*) as well as in hypocotyl cells (*red* and *green circles*)

The fluorescence lifetime of vesicle-located BRI1-EGFP after BL addition

The FLT of plasma membrane-located BRI1-EGFP (Fig. 2 and Electronic Supplementary Material Fig. S2) can be attributed to a BL-induced change in the membrane potential, which might be caused by a BRI1-dependent increase in P-ATPase activity [20]. This is in accordance with recent studies that suggest a more direct function of BRI1, which might be independent of the well-described downstream signaling factors [28]. Previous studies suggest a complex signaling pathway of BRI1 mediated by a manifold of proteins including BRI1 kinase inhibitors and BR signaling kinases in intracellular compartments [29, 30]. It has been noted before that the dual localization of BRI1 both at the plasma membrane and in intracellular vesicles is of importance for its function, recycling, and degradation [31]. However, the BRI1-induced stimulation of the P-ATPase and the subsequent cell-wall expansion [20] may form an additional, independent signaling pathway. To further explore this matter, it is suggested to measure whether a BL-induced lifetime decrease can also be observed for BRI1-EGFP located in the intracellular vesicles. Therefore, we recorded FLIM images of BRI1-EGFP-expressing root cells exposed to 50 nM BL (30× 30 μm^2), applied FIDSAM, and compared the FLT of BRI1-EGFP in the plasma membrane with that of the intracellular vesicles (Fig. 4a, b). Due to the application of FIDSAM, we can exclude the observation of vesicles containing no BRI1-EGFP, which would corrupt reliable and quantitative analysis of the experimental data. As reported previously in a confined cellular area for overexpressed BRI1-EGFP [5], the FLT of plasma membrane-located BRI1-EGFP significantly decreased within 30 min after addition of BL, which is indicative for an alteration in the membrane potential. In sharp contrast, in the FIDSAM-FLIM studies presented here, we observe that the FLT of vesicle-located BRI1-EGFP remained unchanged (Fig. 4a, b). On the one hand, these data indicate that the BL-induced change in the membrane potential—presumably caused by the induction of P-ATPase activity [20]—reflects a rapid and specific function of plasma membrane-located BRI1 [5, 28] and is independent of vesicle-located BRI1-EGFP and the corresponding intracellular signaling pathway. On the other hand, this implicates that the downstream signaling events of the BRI1 response pathway, which postulate its initiation from the vesicle-located hormone receptor [17], do not require electrophysiological processes for, e.g., the BL-dependent gene expression changes. Consequently,

FIDSAM-FLIM allows for the detection and differentiation of several independent but simultaneous signaling pathways.

Conclusion

We presented the application of FIDSAM to different plant cell types (root, hypocotyl, and leaf cells) of transgenic *Arabidopsis* expressing a low-abundant plasma membrane-located protein BRI1-EGFP, which was expressed to only the wild-type levels. We demonstrate the applicability of this method to images exhibiting 80% of background fluorescence by still revealing the 20% of the target BRI1-EGFP signal.

By combination of FLIM with FIDSAM, we convincingly demonstrate that the hormone-induced decrease in fluorescence lifetime is true and can be observed not only in plant cells that ectopically overexpress BRI1-EGFP [5, 20] but also for cells expressing only wild-type levels of the fusion protein.

BRI1-EGFP localizes to discrete domains at the plasma membrane of non-treated cells, which display different membrane potential. After exogenous supply of BL, a change in the membrane potential is observed with different rates for different membrane domains, which is indicative of an altered P-ATPase activity. Cell-wall expansion and FLT decrease show a linear relationship. The slope of the corresponding linear fit represents the local hormone ligand competence of the cell. Our experiments indicate a higher competence for BL in BRI1-EGFP-expressing hypocotyl than in root cells, which is in accordance with previous reports on physiological responses upon BL treatments of the two tissue types [32]. Therefore, the experiments presented here prove the possibility to determine the competence of different cell types to compounds such as hormones by the correlation of different ligand-specific responses.

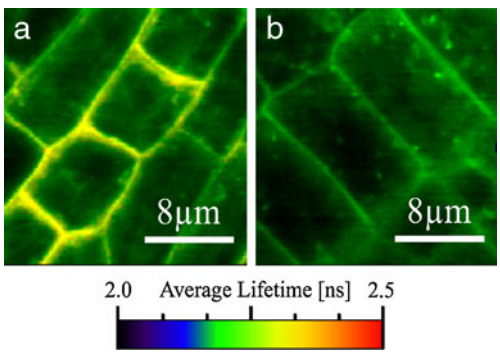

Fig. 4 The fluorescence lifetime of plasma membrane and vesicle-localized BRI1-EGFP behaves different in response to BL. **a** FIDSAM-FLIM image of BRI1-EGFP-expressing *Arabidopsis* root cells before BL addition. **b** FIDSAM-FLIM image of eBRI1-EGFP-expressing *Arabidopsis* root cells 30 min after BL addition

Furthermore, our experiments indicate the existence of at least two independent signaling pathways of BRI1-EGFP: one limited to the plasma membrane and a second including other intracellular compartments as well.

Thus, the combination of FLIM and FIDSAM enables novel insights into subcellular processes at high spatial resolution in living plant cells without the need of protein overexpression.

Materials and methods

Plant material and growth conditions

BRI1-EGFP [17] expressing seedlings were grown for 5 days at 22 °C and under a regime of 14 h light and 10 h darkness on agar plates containing 0.5 Murashige and Skoog media. For measurements without BL addition, seedlings were removed from the plates, transferred onto microscope cover slides, and covered with water and a second microscopic slide. Afterwards, a 50 nM BL solution was applied to the side of the microscopic slide and allowed to diffuse to the seedling.

Optical and spectroscopic measurements

The measurements were performed using a custom built confocal laser-scanning microscope, based on a Zeiss Axiovert [33, 34]. A microscope objective with high numerical aperture (Plan-Neofluar, 100*x*/1.30 oil, Zeiss) was used for focusing the excitation light as well as for collecting the fluorescence emission. The setup was equipped with an avalanche photo diode (PDM series, MicroPhotonDevices (MPD), Italy) as a spectrally integrating detector to record fluorescence intensity. Lifetime decays were recorded using a time-correlated single-photon counting board (PicoHarp 300, Picoquant, Software: SymPhoTime, Picoquant) for data acquisition and the MPD as a detector. Fluorescence intensity images were obtained by raster scanning the sample and detecting emission intensity as well as fluorescence decay trace for every spot on the sampled area. A pulsed 470-nm diode laser (Picoquant LDH-P-C470) operating at a repetition rate of 20 MHz served as an excitation source. The setup was equipped with a 480-nm-long pass filter (Semrock Razor Edge LP02-473RU-25) to block back-scattered excitation light and with a 500-nm bandpass filter (Semrock BrightLine BL500/24) to detect EGFP fluorescence.

Principle of FIDSAM

Label-specific fluorescence (such as EGFP fluorescence) and background fluorescence can be distinguished by the

shape of their fluorescence decay [5]. This property can be used to correct the raw fluorescence image for the background contribution using FIDSAM [6]. In short, FIDSAM utilizes the fact that target fluorescence obeys a well-known, typically monoexponential fluorescence decay whereas fluorescence decays recorded from autofluorescence comprise contributions of a multitude of individual decay statistics and thus are multiexponential. Using a monoexponential decay curve as a reference function, deviations from this reference curve are a direct measure for the autofluorescence contribution and are reflected by the intensity-normalized χ^2 value

$$\chi^2_{norm} = \sum_{k=1}^{n} \frac{\left[N_{norm}(t_k) - N_{c,norm}(t_k)\right]^2}{N(t_k)} \quad (1)$$

which describes the sum of the square deviations of the normalized reference values $N_{c,norm}(t_k)$ from the normalized experimental values $N_{norm}(t_k)$ for every data channel. For pure label fluorescence, ${\chi_{norm}}^2$ approaches 1 [14] and increases with increasing autofluorescence interference. On the basis of these data, the raw image can effectively be corrected for unspecific background luminescence, by dividing each pixel of the raw image by the corresponding ${\chi^2}_{norm}$ value to obtain the corrected image.

Acknowledgements We are grateful to Karin Schumacher for providing the BRI1-GFP line and to Christian Blum for the purified eGFP. This work was supported by a DFG grant to K.H. (HA 2146/10-1) and doctoral and junior group leader fellowships of the state Baden-Württemberg and the University of Tübingen to K.C., K.E., and F.S.

References

1. Westphal V, Rizzoli SO, Lauterbach MA, Kamin D, Jahn R, Hell SW (2008) Video-rate far-field optical nanoscopy dissects synaptic vesicle movement. Science 320:246–249
2. Willig KI, Rizzoli SO, Westphal V, Jahn R, Hell SW (2006) STED microscopy reveals that synaptotagmin remains clustered after synaptic vesicle exocytosis. Nature 440:935–939
3. Betzig E, Patterson GH, Sougrat R, Lindwasser OW, Olenych S, Bonifacino JS, Davidson MW, Lippincott-Schwartz J, Hess HF (2006) Imaging intracellular fluorescent proteins at nanometer resolution. Science 313:1642–1645
4. Schnell SA, Staines WA, Wessendor MW (1999) Reduction of lipofuscin-like autofluorescence in fluorescently labeled tissue. J Histochem Cytochem 47:719–730
5. Elgass K, Caesar K, Schleifenbaum F, Stierhof Y-D, Meixner AJ, Harter K (2009) Novel application of fluorescence lifetime and fluorescence microscopy enables quantitative access to subcellular dynamics in plant cells. PLoS ONE 4(Article No.):e5716
6. Schleifenbaum F, Elgass K, Sackrow M, Caesar K, Berendzen K, Meixner AJ, Harter K (2009) Fluorescence intensity decay shape analysis microscopy (FIDSAM) for quantitative and sensitive live-cell imaging: a novel technique for fluorescence microscopy of endogenously expressed fusion-proteins. Mol Plant 3:555–562. doi:10.1093/mp/ssp110
7. Elgass K, Caesar K, Schleifenbaum F, Meixner AJ, Harter K (2010) The fluorescence lifetime of BRI1-GFP as probe for the noninvasive determination of the membrane potential in living cells. Proc SPIE 7568:756804
8. Nakabayashi T, Wang HP, Kinjo M, Ohta N (2008) Application of fluorescence lifetime imaging of enhanced green fluorescent protein to intracellular pH measurements. Photochem Photobiol Sci 7:668–670
9. van Manen HJ, Verkuijlen P, Wittendorp P, Subramaniam V, van den Berg TK, Roos D, Otto C (2008) Refractive index sensing of green fluorescent proteins in living cells using fluorescence lifetime imaging microscopy. Biophys J 94:L67–L69
10. Pepperkok R, Squire A, Geley S, Bastiaens PIH (1999) Simultaneous detection of multiple green fluorescent proteins in live cells by fluorescence lifetime imaging microscopy. Curr Biol 9:269–272
11. Billinton N, Knight AW (2001) Seeing the wood through the trees: a review of techniques for distinguishing green fluorescent protein from endogenous autofluorescence. Anal Biochem 291:175–197
12. Suhling K, Davis DM, Phillips D (2002) The influence of solvent viscosity on the fluorescence decay and time-resolved anisotropy of green fluorescent protein. J Fluoresc 12:91–95
13. Suhling K, Siegel J, Phillips D, French PMW, Leveque-Fort S, Webb SED, Davis DM (2002) Imaging the environment of green fluorescent protein. Biophys J 83:3589–3595
14. Lakowicz JR (2006) Principles of fluorescence spectroscopy. Springer, Berlin
15. Tsien RY (1998) The green fluorescent protein. Annu Rev Biochem 67:509–544
16. Wang ZY, Seto H, Fujioka S, Yoshida S, Chory J (2001) BRI1 is a critical component of a plasma-membrane receptor for plant steroids. Nature 411:219–219
17. Geldner N, Hyman DL, Wang XL, Schumacher K, Chory J (2007) Endosomal signaling of plant steroid receptor kinase BRI1. Genes Dev 21:1598–1602
18. Clouse SD, Sasse JM (1998) Brassinosteroids: Essential regulators of plant growth and development. Annu Rev Plant Physiol Plant Mol Biol 49:427–451
19. Sanchez-Rodriguez C, Rubio-Somoza I, Sibout R, Persson S (2010) Phytohormones and the cell wall in Arabidopsis during seedling growth. Trends Plant Sci 15:291–301
20. Caesar K, Elgass K, Chen Z, Huppenberger P, Schleifenbaum F, Oecking C, Meixner AJ, Blatt MR, and Harter K (2010) A short brassinolide-regulated response pathway in the plasma membrane of Arabidopsis thaliana. Plant Journal (in press).
21. Medina J, Ballesteros ML, Salinas J (2007) Phylogenetic and functional analysis of Arabidopsis RCI2 genes. J Exp Bot 58:4333–4346
22. Medina J, Catala R, Salinas J (2001) Developmental and stress regulation of RCI2A and RCI2B, two cold-inducible genes of Arabidopsis encoding highly conserved hydrophobic proteins. Plant Physiol 125:1655–1666
23. Mitsuya S, Taniguchi M, Miyake H, Takabe T (2005) Disruption of RCI2A leads to over-accumulation of Na+ and increased salt sensitivity in Arabidopsis thaliana plants. Planta 222:1001–1009
24. Mitsuya S, Taniguchi M, Miyake H, Takabe T (2006) Over-expression of RC12A decreases Na+ uptake and mitigates salinity-induced damages in Arabidopsis thaliana plants. Physiol Plant 128:95–102
25. Navarre C, Goffeau A (2000) Membrane hyperpolarization and salt sensitivity induced by deletion of PMP3, a highly conserved small protein of yeast plasma membrane. EMBO J 19:2515–2524

26. Nylander M, Heino P, Helenius E, Palva ET, Ronne H, Welin BV (2001) The low-temperature- and salt-induced RCI2A gene of Arabidopsis complements the sodium sensitivity caused by a deletion of the homologous yeast gene SNA1. Plant Mol Biol 45:341–352
27. Elgass K, Caesar K, Harter K, Meixner AJ, and Schleifenbaum F (2010) Combining ocFLIM and FIDSAM reveals fast and dynamic physiological responses at subcellular resolution in living plant cells. Journal of Microscopy.
28. Xu WH, Huang J, Li BH, Li JY, Wang YH (2008) Is kinase activity essential for biological functions of BRI1? Cell Res 18:472–478
29. Wang XL, Chory J (2006) Brassinosteroids regulate dissociation of BKI1, a negative regulator of BRI1 signaling, from the plasma membrane. Science 313:1118–1122
30. Tang WQ, Kim TW, Oses-Prieto JA, Sun Y, Deng ZP, Zhu SW, Wang RJ, Burlingame AL, Wang ZY (2008) BSKs mediate signal transduction from the receptor kinase BRI1 in Arabidopsis. Science 321:557–560
31. Otegui MS, Spitzer C (2008) Endosomal functions in plants. Traffic 9:1589–1598
32. Teale WD, Ditengou FA, Dovzhenko AD, Li X, Molendijk AM, Ruperti B, Paponov I, Palme K (2008) Auxin as a model for the integration of hormonal signal processing and transduction. Mol Plant 1:229–237
33. Blum C, Stracke F, Becker S, Mullen K, Meixner AJ (2001) Discrimination and interpretation of spectral phenomena by room-temperature single-molecule spectroscopy. J Phys Chem A 105:6983–6990
34. Schleifenbaum F, Blum C, Elgass K, Subramaniam V, Meixner AJ (2008) New Insights into the Photophysics of DsRed by Multiparameter Spectroscopy on Single Proteins. J Phys Chem B 112:7669–7674